2021 IEEE International Joint Conference on Biometrics (IJCB) | 978-1-6654-3780-6/21/$31.00 ©2021 IEEE | DOI: 10.1109/IJCB52358.2021.9484401

Finger Vein Verification using Intrinsic and Extrinsic Features

Liying Lin†, Haozhe Liu†, Wentian Zhang, Feng Liu*, Zhihui Lai
[1] Computer Vision Institute, College of Computer Science and Software Engineering,
[2] SZU Branch, Shenzhen Institute of Artificial Intelligence and Robotics for Society
[3] National Engineering Laboratory for Big Data System Computing Technology
[4]Guangdong Key Laboratory of Intelligent Information Processing,
Shenzhen University, Shenzhen 518060, China
{linliying2019, liuhaozhe2019}@email.szu.edu.cn, zhangwentianml@gmail.com,
feng.liu@szu.edu.cn, lai_zhi_hui@163.com

Abstract

Finger vein has attracted substantial attention due to its good security. However, the variability of the finger vein data will be caused by the illumination, environment temperature, acquisition equipment, and so on, which is a great challenge for finger vein recognition. To address this problem, we propose a novel method to design an end-to-end deep Convolutional Neural Network (CNN) for robust finger vein recognition. The approach mainly includes an Intrinsic Feature Learning (IFL) module using an auto-encoder network and an Extrinsic Feature Learning (EFL) module based on a Siamese network. The IFL module is designed to estimate the expectation of intra-class finger vein images with various offsets and rotation, while the EFL module is constructed to learn the inter-class feature representation. Then, robust verification is finally achieved by considering the distances of both intrinsic and extrinsic features. We conduct experiments on two public datasets (i.e. SDUMLA-HMT and MMCBNU_6000) and an in-house dataset (MultiView-FV) with more deformation finger vein images, and the equal error rate (EER) is 0.47%, 0.1%, and 1.69% respectively. The comparison against baseline and existing algorithms shows the effectiveness of our proposed method.

1. Introduction

With the increasing demand of reliable and secure personal identification systems, finger vein verification has attracted widespread attention [1]. Since the structure of the blood vessels is unique to each individual and the shape of the veins no longer changes in adults, finger veins are unique and stable when used to identify. On the other side, as its property of the internal blood vessel, finger vein identification systems are hard to be forged [2]. Thus, it is very successful for the application of finger vein recognition to various industries, such as Banking, finance, government, national security [3] .

A great number of studies have been devoted to the field of finger vein recognition. Most traditional finger vein recognition systems use hand-craft features. Generally, it can be roughly divided into the following three categories:

- Finger vein pattern-based methods. The structure from blood vessels under the skin provides extensive information, which can be regarded as finger vein patterns. A lot of pattern-based methods were conducted for finger vein verification. Miura et al. [4] proposed a method that extracts the finger-vein pattern from the unclear image by using line tracking that starts from various positions. Experimental results show that it achieves robust pattern extraction. Later, in [5], a modified repeated line tracking method was proposed to verify the finger vein image by calculating the maximum curvature. However, the number of iterations of the repetitive linear tracking method directly affects the calculation speed and the results of finger vein extraction.
- Finger vein texture-based methods. Some finger vein texture-base human identification studies [6, 7, 8, 9] were conducted, which considers the grey-scale distribution of finger-vein image pixels. In [6], the authors proposed a local binary pattern which focused on local patterns in various directions. Yang et al. [7] proposed a method based on a personalized best bit map and achieved high robustness and reliability. Furthermore, local derivative pattern [8], local line binary pattern [9] were also exploited to extract the finger vein

†Equal Contribution
*Corresponding Author

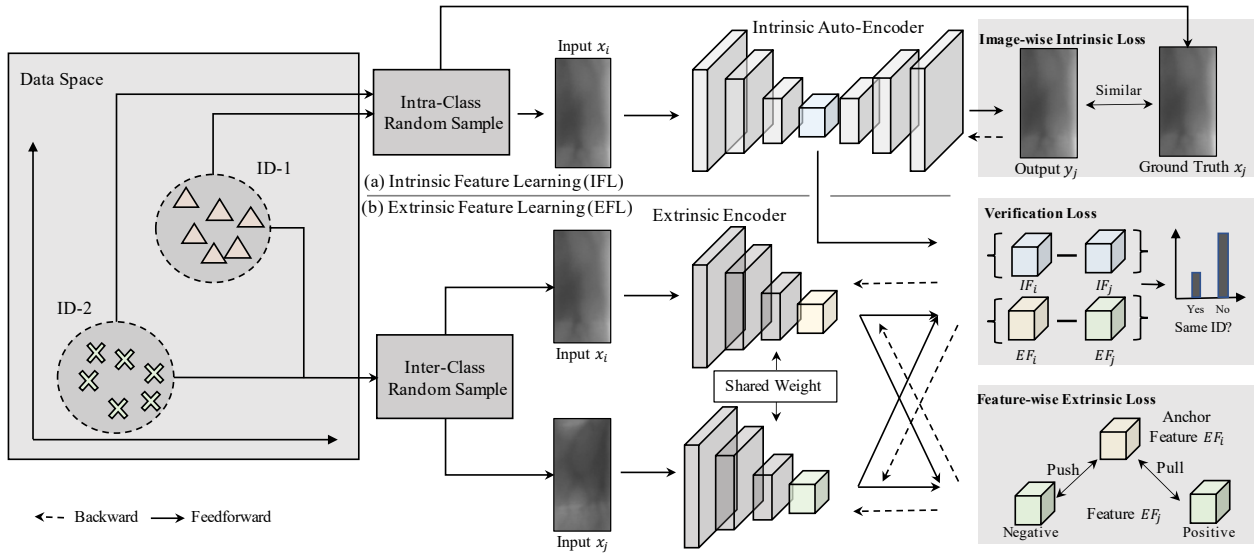

Figure 1. The pipeline of the proposed finger vein verification method, denoted as EI-Verf. EI-Verf consists of two modules: (a) Intrinsic Feature Learning (IFL) module and (b) Extrinsic Feature Learning (EFL) module.

features. This kind of methods have significant advantages such as fast calculation, gray scale invariance and rotation invariance, but still can not effectively extract some vague veins of the low quality images.

- Finger vein minutiae-based methods. Inspired by the bifurcation points and endpoints in the finger vein verification, the methods of extracted finger vein feature base minutiae point were suggested. Qin et al. [10]presented a new scheme to improve the performance of finger-vein identification systems by combining the finger-vein shape, orientation and SIFT features. Peng et al. [11] designed an 8-way filter which selects the parameters of the Gabor filter to extract the finger-vein features and utilize the scale-invariant feature transform features to offset the effect of image rotation and shift impact.

Although the above methods extract effective features of finger veins to some extent, they still cannot solve the problem of image variation among different individuals. In recent years, benefitting from the improvement of computing power, deep learning-based image recognition methods are being applied to the finger vein field. For example, Radzi et al. [12] proposed a method that only used four-layer CNN (convolutional neural network) for finger vein recognition. Huang et al. [13] proposed a DeepVein for finger vein verification based on deep CNNs. Fang et al. [14] designed a lightweight two-channel and two-stream network to solve the displacement problem by extracting the mini-ROI from the original image. However, these models were designed to learn inter-class difference but ignore the intra-class difference, resulting in degraded performance to images with variations.

Considering the problem mentioned above, a novel finger vein verification system, which consists of an Intrinsic Feature Learning (IFL) module and an Extrinsic Feature Learning (EFL) module, is constructed. Specifically, the images with the same ID are randomly sampled as a pair to train the IFL module. Thus, the IFL module based an auto-encoder network is designed to learn the finger vein features from the same ID. Furthermore, a deep Siamese network is employed in the EFL module. Unlike sampling from the same ID in IFL, the pair-wise images with random IDs are used in EFL to extract inter-class features. Then, the distinguishable features extracted from the above two modules were both used to calculate distances and fed into the logistic regression model for verification. We implement our approach on two public datasets and an in-house dataset with the close-set protocol in [14], the performance of EERs demonstrates the effectiveness of the proposed method.

2. Finger Vein Verification using EI-Verf Model

Based on the idea of that a good classifier should try to make the intra-class gap be small and the inter-class gap be large, we proposed an EI-Verf model to extract intra- and inter-class features for vein verification. The principles of the proposed method are illustrated in Fig. 1. In our method, an Intrinsic Feature Learning (IFL) module based on an auto-encoder network is designed to estimate the expectation of intra-class vein images by randomly reconstructing images sampled from the selected ID groups. Meanwhile, an Extrinsic Feature Learning (EFL) module

Table 1. Specification for the Network Structure used in Proposed Method.

	Layer type	Number	Channel	Input size	Output size
Res-Block	Conv3×3 (with BN, Relu)	1	-	-	-
	Conv3×3 (with BN)	1	-	-	-
	shortcut from input using Conv1×1 (with BN)				
	Conv3×3 (with BN, Relu)	1	-	-	-
	Conv3×3 (with BN)	1	-	-	-
Transpose-Block	Transpose Conv2×2	1	-	-	-
	Conv3×3	1	-	-	-
Encoder ($F_I(\cdot)$,$F_E(\cdot)$)	Conv7×7	1	64	**64×128×1**	32×64×64
	Max Pooling	1	-	32×64×64	16×32×64
	Conv3×3	4	64	16×32×64	16×32×64
	Res-Block	3	(128, 256, 512)	16×32×64	2×4×512
Decoder ($F_D(\cdot)$)	Transpose-Block	5	(512, 256, 128, 64, 64)	2×4×512	64×128×64
	Conv1×1	1	1	64×128×64	**64×128×1**

based on a Siamese network is proposed to learn the inter-class feature representation. Finally, finger vein verification can be achieved by hierarchically calculating the match score which represents distances of extrinsic and intrinsic features. In the following subsections, we will detailedly introduce the IFL and EFL modules of the proposed method, and then present the verification based on the extracted features from IFL and EFL modules.

2.1. Intrinsic Feature Learning (IFL)

During the process of capturing finger veins, slight offsets and rotations are ubiquitous, resulting in a large intra-class distance. In order to minimize the intra-class distance for more accurate verification, a generative model based IFL module is proposed to embed the intra-class samples with various offsets and rotation into a stable representation. Specifically, given a set of finger vein images, $X^t = \{x_0^t, ..., x_i^t, ..., x_n^t\}$, with the same ID t, two images, (x_i^t, x_j^t), are randomly sampled as a pair-wise data to train Intrinsic Auto-Encoder $F_{AE}(\cdot)$ by minimizing image-wise intrinsic loss, $\mathcal{L}_r(x_i, x_j)$,

$$F_{AE}(x_i^t) = F_D(F_I(x_i^t)) \tag{1}$$

$$\mathcal{L}_r(x_i^t, x_j^t) = ||F_{AE}(x_i^t) - x_j^t||_2 \tag{2}$$

where $F_I(\cdot)$ is the encoder and $F_D(\cdot)$ is the decoder of Intrinsic Auto-Encoder. Since x_j^t is randomly selected from X^t rather than x_i^t, $\mathbb{E}_{x_i \sim X^t}$ is the surrogate of the ground truth for each $x_i^t \in X^t$. Based on this observation, a stable intrinsic representation IF_i , for verification, can be obtained by,

$$IF_i = F_I(x_i^t) \tag{3}$$

Since the same input x_i corresponds to different x_j, the convergence speed of $F_{AE}(\cdot)$ may be decreased. Thus, an U-shape architecture is adopted in $F_{AE}(\cdot)$ to facilitate training procedure. As listed in Table 1, ResNet-18 is used as the encoder of Intrinsic Auto-Encoder, consisting of a convolution layer with 7×7 kernel, a max pooling layer, four 3×3 convolution layers and three Res-Blocks. While, the decoder is composed of five Transpose-Blocks and a convolution layer with 1×1 kernel.

2.2. Extrinsic Feature Learning (EFL)

As IFL module is guided to extract intrinsic features, EFL module should embed the vein images into extrinsic codes to complement the limitation caused by single-level features. To achieve this goal, a deep siamese network $F_E(\cdot)$ is applied in EFL module. The architecture of $F_E(\cdot)$ is the same with F_I, but the types of input are quite different. Unlike sampling from the same ID in IFL, the pair-wise images $(x_i^{t_0}, x_j^{t_1})$ with random IDs are used in EFL module to learn inter-class features. Specifically, a pull-push game, namely feature-wise intrinsic loss $\mathcal{L}_p(x_i^{t_0}, x_j^{t_1})$, is used to train $F_E(\cdot)$, as shown below

$$\mathcal{L}_p(x_i, x_j) = \begin{cases} \max(\mathcal{L}_d(EF_i, EF_j) - m_p, 0), & t_0 = t_1 \\ \max(m_q - \mathcal{L}_d(EF_i, EF_j), 0), & t_0 \neq t_1 \end{cases}$$

$$\mathcal{L}_d = (EF_i, EF_j) = ||EF_i - EF_j||_2 \tag{4}$$

where m_p and m_q are the predefined threshold for dynamic adaption and EF_i is the embedding code of $F_E(x_i^{t_0})$. In $\mathcal{L}_p(x_i, x_j)$, genuine pairs are pulled as the similar representation, while imposter pairs are pushed for learning discriminative features.

2.3. Vein Verification using Intrinsic and Extrinsic Features

Unlike IF_i concentrating on the intrinsic features from the same IDs, EF_i pays more attention to the discriminative feature among different IDs. Consequently, IF_i and EF_i are complementary for verification. We then defined a

Table 2. Summary of Experiment Configurations

	Institution	Details				Protocol
		Subject/Image Num.	Captured Finger	Sensor	Resolution	
SDUMLA-HMT (DB-1)	Shandong University	106/3816	index, middle and ring finger	single camera	320×240	Fang et al. [14]
MMCBNU_6000 (DB-2)	Chonbuk National University	100/6000	index, middle and ring finger	single camera	640×480	Fang et al. [14]
MultiView-FV (DB-3)	SZU-CVI	135/6480	index and middle finger	multiple cameras	1280×1024	close-set

match score $\hat{s}_{ij}$ based on the distance between $\{IF_i, EF_i\}$ and $\{IF_j, EF_j\}$, as shown in Equation 6.

$$\hat{s}_{ij} = \frac{1}{1 + exp(-W^{\top} A_{ij})} \tag{5}$$

$$A_{ij} = \{A_i, A_j\} = \{\mathcal{L}_d(IF_i, IF_j), \mathcal{L}_d(EF_i, EF_j)\} \tag{6}$$

where W is a learnable parameter, and can be updated by verification loss

$$\mathcal{L}_c(x_i, x_j) = s_{ij} log(\hat{s}_{ij}) + (1 - s_{ij}) log(1 - \hat{s}_{ij})$$
$$s_{ij} = \begin{cases} 0 & ID\ t_i = ID\ t_j \\ 1 & ID\ t_i \neq ID\ t_j \end{cases} \tag{7}$$

Among them, s_{ij} is the ground truth of $\hat{s}_{ij}$.

It should be noted that in order to obtain more discriminative features among different IDs, $F_E(\cdot)$ is also trained by $\mathcal{L}_c(x_i, x_j)$, and the learning objective of $F_E(\cdot)$ is finally presented as $\mathcal{L}_c$+$\mathcal{L}_p$ in this paper. We summarized the proposed EI-Verf Model in Algorithm.1.

Algorithm 1 EI-Verf

Input:
Training Samples: $\{X^t | t \in N\}$
Test Samples: x_i and x_j
Initialization of $F_{AE}(\cdot)$ and $F_E(\cdot)$

Output:
Trained CNNs: $F_I(\cdot)$ and $F_E(\cdot)$ //$F_I(\cdot)$ is the encoder of $F_{AE}(\cdot)$
Match score $\hat{s}_{ij}$ of xt_i and x_j

for all training steps **do**
  Calculate image-wise intrinsic loss $\mathcal{L}_r$ according to Eq. (2)
  Obtain feature IF using IFS Module according to Eq. (3)
  Derive feature EF by $F_E(\cdot)$;
  Calculate feature-wise extrinsic loss $\mathcal{L}_p$ according to Eq. (4)
  Calculate distance metric A by Eq.(6)
  Calculate verification loss $\mathcal{L}_c$ according to Eq. (7)
  Update $F_{AE}(\cdot)$ based on $\frac{\partial \mathcal{L}_r}{\partial F_{AE}}$ and update $F_E(\cdot)$ by $\frac{\partial (\mathcal{L}_p + \mathcal{L}_c)}{\partial F_E}$
end for
Obtain A_i and A_j of x_i and x_j by $F_E(\cdot)$ and $F_I(\cdot)$.
Obtain match score $\hat{s}_{ij}$ by Eq. (5)
Return $\hat{s}_{ij}$, $F_I(\cdot)$ and $F_E(\cdot)$

3. Experimental Results and Analysis

To evaluate the performance of the proposed method, in this section, extensive experiments were carried on public datasets namely SDUMLA-HMT and MMCBNU_6000, and one in-house dataset established by ourselves, denoted as MultiView-FV[1]. We firstly introduced the datasets and implementation details in subsection 3.1. Subsection 3.2. then proved the effectiveness of the proposed EI-Verf model. Comparison with current vein verification methods was finally shown in subsection 3.3.

3.1. Datasets and Implementation Details

As listed in Table 2, three datasets, including SDUMLA-HMT [15], MMCBNU_6000 [16] and MultiView-FV, are used to test the performance of verification. In particular, SDUMLA-HMT is collected by Shandong University, which consists of 106 subjects. As a total, 13356 pairs with 3816 vein images are used for training and test. The protocol given in [14] is adopted in this paper, where 10176 pairs are employed as training set, and the other pairs are used as test set. The samples of this dataset are given in Fig. 2(a). In MMCBNU_6000, 100 subjects with 6000 vein images are collected. 6 fingers are imaged from each subject and 10 images are captured from each finger. Some samples are shown in Fig. 2(b). The protocol of data partition given in [14] is also adopted in this paper. For each subject, the first 5 samples are used as training samples, and the others are adopted as test samples. It should be noted that most of the images included in the aforementioned datasets have small variations between images with the same ID by our observation. This characteristic of these two public datasets can not effectively test the robustness of verification methods against the slight off-sets and rotations in practice. Thus, a new dataset, denoted as MultiView-FV, is collected by our-

[1] https://github.com/CV-SZU/A-challenging-benchmark-dataset-with-multiview-finger-vein-images

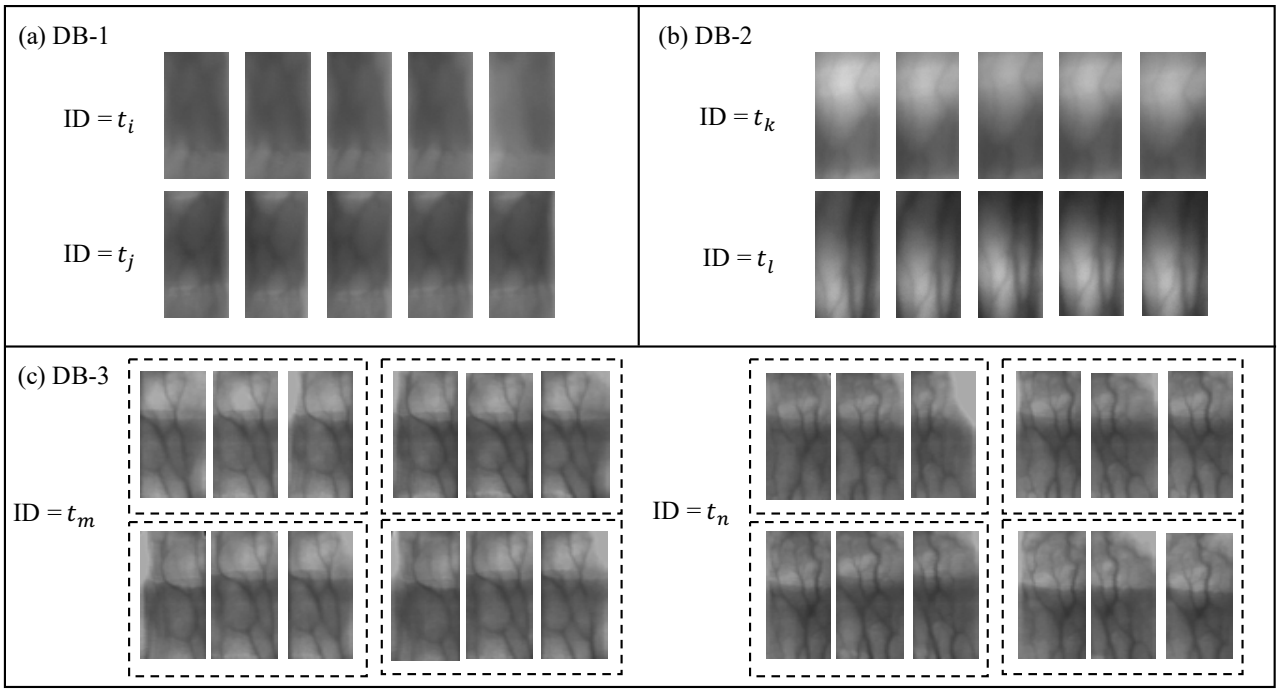

Figure 2. The samples of finger veins in three datasets. (a) is the samples captured from DB-1, i.e. SDUMLA-HMT, (b) refer to the samples from DB-2, MMCBNU_6000, and (c) corresponds to the data collected in MultiView-FV.

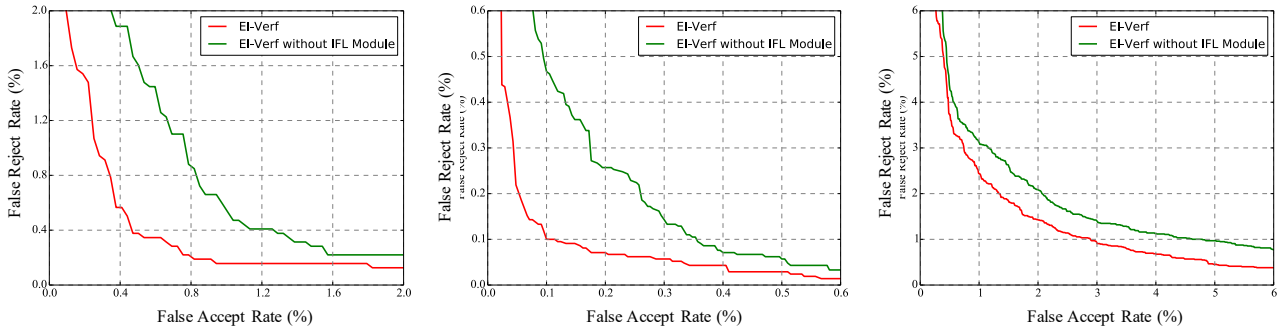

(a) EER Curve Carried on DB-1 (b) EER Curve Carried on DB-2 (c) EER Curve Carried on DB-3

Figure 3. EERs curves of the proposed method carried on (a) SDUMLA-HMT(DB-1) , (b) MMCBNU_6000 (DB-2) and (c) MultiView-FV (DB-3). Green curves refer to the results of the proposed method without IFL Module, while red curves are the cases using both intrinsic and extrinsic features.

selves in this paper. Different from existing datasets, multi-view finger vein images of one finger are captured by multiple cameras at the same time using the device shown in Fig. 4. The samples of finger veins in MultiView-FV dataset are given in Fig. 2(c). As given in Table 2, there are 6480 finger vein images captured from 135 individuals, each subject provided images of his/her index and middle finger of both hands, and the collection for each finger is repeated for 4 times to obtain 12 finger vein images. Therefore, without alignment and rotation-specific operations, MultiView-FV provides a challenging benchmark to test the performance of verification in practice. Like the image pair combination approach in [14] , 6 images from the same finger are randomly selected for training, and the remaining 6 images are used for test in this dataset.

Our implementation is based on the public platform pytorch. We initialized the weights in each layer from the model pretrained in ImageNet. The Adam optimizer is used for our method, the learning rate is set to 0.001. Momentum and gamma of scheduler stepLR are set to 0.9 and 0.1, respectively. Data preprocessing techniques, including normalization and Gabor filter are employed to enhance the texture of finger vein images. Our work station's CPU is 2.8GHz, RAM is 32GB and GPU is NVIDIA TITAN RTX.

Table 3. Performance of EI-Verf Model using Different Backbones and Proposed Modules in terms of Equal Error Rate (%) with Various Datasets.

Backbone for $F_I(\cdot)$ and $F_E(\cdot)$	EFL Module	IFL Module	Datasets EER.(%)			
			SDUMLA-HMT (DB-1)	MMCBNU_6000 (DB-2)	MultiView-FV (DB-3)	Mean $\pm$ s.d.
Resnet-18 [20]	✓	×	0.85	0.24	2.06	1.05 ± 0.76
	✓	✓	**0.47**	**0.1**	**1.69**	$\mathbf{0.76 \pm 0.68}$

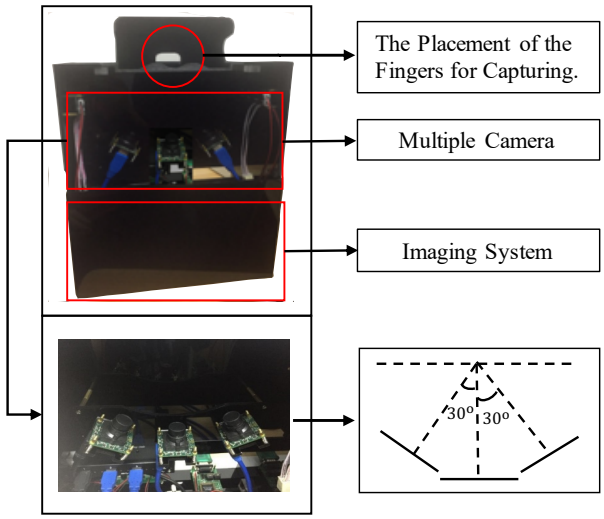

Figure 4. The finger vein reader of MultiView-FV, consisting of the placement of the fingers, multiple cameras and the imaging system. The angle among the adjacent cameras is 30^o

To evaluate the performance of the methods, Equal Error Rate (EER) is used in this paper. EER reflects the verification performance of the method, which is the rate when FAR equaling FRR. The smaller the value of EER, the better the performance of the method. For camparison, approaches of Xie et al. [17], Liu et al. [18], Qiu et al. [19] and Fang et al. [14] are employed in this paper.

3.2. Effectiveness Validation of the Proposed EI-Verf Model

To quantify the contribution of the intrinsic features for verification, we tested the discriminative performance of the method with or without IFL Module. As the results shown in Table 3, the better performance, carried on all of the datasets, can be achieved by the proposed method, when adopting IFL module. In particular, the proposed method with IFL Module can achieve 0.47% EER in DB-1, while the EER of EFL module can only reach to 0.85%, which proves the effectiveness of the IFL module. EER curves with more detailed information are shown in Fig.3. As shown in the figure, EERs in differerent datasets are all smaller than the cases without IFL Module, which further proves the importance of intrinsic features for robust verification.

Table 4. Performance Comparison Between the Proposed Method and State of the Art Methods in terms of Equal Error Rate(%).

	SDUMLA-HMT (DB-1)	MMCBNU_6000 (DB-2)	MultiView-FV (DB-3)
Xie et al. [17] (2014)	**0.47**	0.4	-
Liu et al. [18] (2016)	-	0.3	-
Qiu et al. [19] (2016)	1.59	-	-
Fang et al. [14] (2018)	**0.47**	**0.1**	4.65
Proposed method	**0.47**	**0.1**	**1.69**

3.3. Comparison with Existing Methods

To further verify the effectiveness of the proposed method, we compared it with four state-of-the-art methods, i.e. [17, 18, 19, 14], as shown in Table 4. It should be noted that, MultiView-FV is a new collected dataset. Thus, we repeated the existing best method in [14] as the baseline to test the performance of the proposed method. In DB-1 and DB-2, the proposed method can achieve 0.47% and 0.1% EER respectively. In DB-3, since the images with various rotation and offsets are considered, the competing methods can be test effectively in a more challenging case. Compared with the baseline, a 2.96% improvement of EER can be achieved by the proposed method. This indicates the proposed EI-Verf is more robust agianst offsets and rotations, and is more suitable in practical applications.

4. Conclusion

In this paper, an effective method called EI-Verf was proposed for finger vein verification. Intra-class and Inter-class features can be well learned by the designed IFL and EFL modules. Robust verification was finally achieved by considering the distances of both intrinsic and extrinsic features. The experimental results showed that our proposed method has achieved comparable EER with the existing methods on the public datasets. An improvement of 2.96% was obtained when evaluated on the in-house dataset with more deformation finger vein images, which demonstrated the robustness and effectiveness of the proposed method. Our future work can be extended to reduce the size of the model for real application, and data augmentation will be considered to further improve performance.

Acknowledgment

The work is partially supported by the National Natural Science Foundation of China under grants no. 62076163

and 91959108, the Shenzhen Fundamental Research fund JCYJ20190808163401646, JCYJ20180305125822769 and Tencent "Rhinoceros Birds"-Scientific Research Foundation for Young Teachers of Shenzhen University.

References

[1] Kalsoom Fatima, Sumbal Nawaz, and Sobia Mehrban. Biometric authentication in health care sector: a survey. In *2019 International Conference on Innovative Computing*, pages 1–10. IEEE, 2019.

[2] Gongping Yang, Rongyang Xiao, Yilong Yin, and Lu Yang. Finger vein recognition based on personalized weight maps. *Sensors*, 13(9):12093–12112, 2013.

[3] Rig Das, Emanuela Piciucco, Emanuele Maiorana, and Patrizio Campisi. Convolutional neural network for finger-vein-based biometric identification. *IEEE Transactions on Information Forensics and Security*, 14(2):360–373, 2018.

[4] Naoto Miura, Akio Nagasaka, and Takafumi Miyatake. Feature extraction of finger-vein patterns based on repeated line tracking and its application to personal identification. *Machine vision and applications*, 15(4):194–203, 2004.

[5] Naoto Miura, Akio Nagasaka, and Takafumi Miyatake. Extraction of finger-vein patterns using maximum curvature points in image profiles. *IEICE TRANSACTIONS on Information and Systems*, 90(8):1185–1194, 2007.

[6] Timo Ojala, Matti Pietikainen, and Topi Maenpaa. Multiresolution gray-scale and rotation invariant texture classification with local binary patterns. *IEEE Transactions on pattern analysis and machine intelligence*, 24(7):971–987, 2002.

[7] Gongping Yang, Xiaoming Xi, and Yilong Yin. Finger vein recognition based on (2d) 2 pca and metric learning. *Journal of Biomedicine and Biotechnology*, 2012, 2012.

[8] Eui Chul Lee, Hyunwoo Jung, and Daeyeoul Kim. New finger biometric method using near infrared imaging. *Sensors*, 11(3):2319–2333, 2011.

[9] Yu Lu, Sook Yoon, Shan Juan Xie, Jucheng Yang, Zhihui Wang, and Dong Sun Park. Finger vein recognition using generalized local line binary pattern. *KSII Transactions on Internet & Information Systems*, 8(5), 2014.

[10] Huafeng Qin, Lan Qin, Lian Xue, Xiping He, Chengbo Yu, and Xinyuan Liang. Finger-vein verification based on multi-features fusion. *Sensors*, 13(11):15048–15067, 2013.

[11] Jialiang Peng, Ning Wang, Ahmed A Abd El-Latif, Qiong Li, and Xiamu Niu. Finger-vein verification using gabor filter and sift feature matching. In *2012 Eighth International Conference on Intelligent Information Hiding and Multimedia Signal Processing*, pages 45–48. IEEE, 2012.

[12] Syafeeza Ahmad Radzi, Mohamed Khalil Hani, and Rabia Bakhteri. Finger-vein biometric identification using convolutional neural network. *Turkish Journal of Electrical Engineering & Computer Sciences*, 24(3):1863–1878, 2016.

[13] Houjun Huang, Shilei Liu, He Zheng, Liao Ni, Yi Zhang, and Wenxin Li. Deepvein: Novel finger vein verification methods based on deep convolutional neural networks. In *2017 IEEE International Conference on Identity, Security and Behavior Analysis*, pages 1–8. IEEE, 2017.

[14] Yuxun Fang, Qiuxia Wu, and Wenxiong Kang. A novel finger vein verification system based on two-stream convolutional network learning. *Neurocomputing*, 290:100–107, 2018.

[15] Yilong Yin, Lili Liu, and Xiwei Sun. Sdumla-hmt: a multimodal biometric database. In *Chinese Conference on Biometric Recognition*, pages 260–268. Springer, 2011.

[16] Yu Lu, Shan Juan Xie, Sook Yoon, Zhihui Wang, and Dong Sun Park. An available database for the research of finger vein recognition. In *2013 6th International congress on image and signal processing*, volume 1, pages 410–415. IEEE, 2013.

[17] Shan Juan Xie, Sook Yoon, Jucheng Yang, Yu Lu, Dong Sun Park, and Bin Zhou. Feature component-based extreme learning machines for finger vein recognition. *Cognitive Computation*, 6(3):446–461, 2014.

[18] Chenguang Liu and Yeong-Hwa Kim. An efficient finger-vein extraction algorithm based on random forest regression with efficient local binary patterns. In *2016 IEEE International Conference on Image Processing*, pages 3141–3145. IEEE, 2016.

[19] Shirong Qiu, Yaqin Liu, Yujia Zhou, Jing Huang, and Yixiao Nie. Finger-vein recognition based on dual-sliding window localization and pseudo-elliptical transformer. *Expert Systems with Applications*, 64:618–632, 2016.

[20] Kaiming He, Xiangyu Zhang, Shaoqing Ren, and Jian Sun. Deep residual learning for image recognition. In *Proceedings of the IEEE conference on computer vision and pattern recognition*, pages 770–778, 2016.